Aquat Geochem (2013) 19:147–171
DOI 10.1007/s10498-012-9185-0

ORIGINAL PAPER

Contribution of P_{CO_2eq} and $^{13}C_{TDIC}$ Evaluation to the Identification of CO_2 Sources in Volcanic Groundwater Systems: Influence of Hydrometeorological Conditions and Lava Flow Morphologies—Application to the Argnat Basin (Chaîne des Puys, Massif Central, France)

Guillaume Bertrand · Hélène Celle-Jeanton · Sébastien Loock · Frédéric Huneau · Véronique Lavastre

Received: 14 June 2012 / Accepted: 27 December 2012 / Published online: 20 January 2013

Abstract Mineralization of groundwater in volcanic aquifers is partly acquired through silicates weathering. This alteration depends on the dissolution of atmospheric, biogenic, or mantellic gaseous CO_2 whose contributions may depend on substratum geology, surface features, and lava flow hydrological functionings. Investigations of P_{CO_2eq} and $\delta^{13}C_{TDIC}$ (total dissolved inorganic carbon) on various spatiotemporal scales in the unsaturated and saturated zones of volcanic flows of the Argnat basin (French Massif Central) have been

G. Bertrand (✉) · V. Lavastre
Laboratoire Magmas et Volcans, Université de Lyon, Université Jean Monnet,
23 rue du Dr. Michelon, 42023 Saint Etienne, France
e-mail: guillaume.bertrand@email.com

V. Lavastre
e-mail: veronique.lavastre@univ-st-etienne.fr

G. Bertrand · H. Celle-Jeanton · S. Loock · V. Lavastre
CNRS, UMR 6524, LMV, 63038 Clermont-Ferrand, France
e-mail: h.celle-jeanton@opgc.univ-bpclermont.fr

S. Loock
e-mail: loock@unice.fr

G. Bertrand · H. Celle-Jeanton · S. Loock · V. Lavastre
IRD, R 163, LMV, 63038 Clermont-Ferrand, France

H. Celle-Jeanton · S. Loock
Laboratoire Magmas et Volcans, Clermont Université, Université Blaise Pascal,
BP 10448, 5, rue Kessler, 63000 Clermont-Ferrand, France

F. Huneau
Laboratoire d'Hydrogéologie, Faculté des Sciences et Techniques, Université de Corse Pascal Paoli,
Campus Grimaldi, BP 52, 20250 Corte, France
e-mail: huneau@univ-corse.fr

F. Huneau
CNRS, UMR 6134, SPE, 20250 Corte, France

carried out to identify the carbon sources in the system. Mantellic sources are related to faults promoting CO_2 uplift from the mantle to the saturated zone. The contribution of this source is counterbalanced by infiltration of water through the unsaturated zone, accompanied by dissolution of soil CO_2 or even atmospheric CO_2 during cold periods. Monitoring and modeling of $\delta^{13}C_{TDIC}$ in the unsaturated zone shows that both P_{CO_2eq} and $\delta^{13}C_{TDIC}$ are controlled by air temperature which influences soil respiration and soil-atmosphere CO_2 exchanges. The internal geometry of volcanic lava flows controls water patterns from the unsaturated zone to saturated zone and thus may explain $\delta^{13}C$ heterogeneity in the saturated zone at the basin scale.

Keywords Volcano · Unsaturated zone · Groundwater · P_{CO_2} · Carbon-13

1 Introduction

Volcanic aquifers are increasingly under interest and studied from a hydrogeochemical point of view for two main reasons. At first, volcanic groundwater use is vital in many locations around the world (Stieljes 1988; Violette et al. 1997; Cruz and Amaral 2004; Dafny et al. 2006; Demlie et al. 2008; D'Ozouville et al. 2008; Bertrand et al. 2010; Charlier et al. 2011) including in developing countries (Kulkarni et al. 2000; Carrillo-Rivera et al. 2007; Demlie et al. 2008). Therefore, volcanic aquifer managements and international policies implementations (e.g., Groundwater Directive from the European Union 2006/118/EC, European Parliament 2006) or the protection of groundwater-dependent ecosystems (Kløve et al. 2011; Bertrand et al. 2012a, b) imply the assessment of their spatial and temporal hydrochemical patterns in order to evaluate their possible fates in a context of local and global anthropogenic pressures. Secondly, as shown in pioneering works (Garrels and Mackenzie 1971), the weathering of silicates, in particular, is one of the major processes affecting the global carbon cycle through silicates–water–CO_2 interaction, leading, in the long term, to carbonate precipitation and sedimentation in the oceans. In order to quantify this interaction, many studies have focused on river geochemistry on a global (Stallard and Edmond 1983; Meybeck 1987; Négrel et al. 1993; Edmond et al. 1995; Gaillardet et al. 1999) and smaller scale (Bluth and Kump 1994; White and Blum 1995; Gislason et al. 1996; Louvat and Allègre 1997; Stewart et al. 2001; Millot et al. 2002). Amiotte-Suchet and Probst (1993) highlighted the importance of lithology and showed that basalts are among the most easily weathered crystalline silicate rocks. Gaillardet et al. (1999) determined that the atmospheric CO_2 consumption flux derived from basalts weathering represents 30 % of the global flux from all silicates. Thus, basalt weathering acts as an important regulator of Earth's climate on a geological time scale (Dessert et al. 2003), and basaltic systems are now viewed to be potential zone of CO_2 injection for greenhouse effect limitation (Matter et al. 2007 and references therein).

As a result, numerous studies were devoted to identify factors affecting CO_2 fates through basalt weathering and focused on geochemical factors such as rock mineralogy and age, runoff and infiltration rates, temperature, and vegetation (e.g., Nesbitt and Wilson 1992; Gislason et al. 1996; Stefansson and Gislason 2001 and references therein; Pokrovsky et al. 2005; Lloret et al. 2011; Benedetti et al. 1994; Drever 1994; White and Blum 1995; Gislason et al. 1996; Brady et al. 1999; Moulton et al. 2000; Dessert et al. 2001; Hinsinger et al. 2001).

In addition, a particularity of volcanic areas is that mantellic or metamorphic CO_2 may interact with these systems, sometimes constituting the major source of carbon in volcanic aquifers (Alley 1993; Rose et al. 1996; Federico et al. 2002; Chiodini et al. 1999; Martin-Del Pozzo et al. 2002; Karakaya et al. 2007), and modifying the CO_2 patterns.

However, these studies addressed only partially two factors that could play a significant role in carbon patterns at the lava flow scale. Primarily, the patterns of biogenic and atmospheric CO_2 dissolving in unsaturated zones depend on soil structure and microclimate (Dudziak and Halas 1996; Lohila et al. 2007) which are parameters changing at a little time scale. Gislason et al. (1996) addressed partially this topic by analyzing the effect of snow cover on weathering rates and showed that this process decreases as snow cover increases, but the underlying processes were not investigated temporally. Secondly, the effects of morphological particularities of lava flows were not investigated in detail. Internal geometry of rocks influences water dynamics (Kiernan et al. 2003; Dafny et al. 2006) which may significantly affect the ways and the rate in which the CO_2 is consumed (Pacheco and Van der Weijden 2012 and references therein).

In order to fill these gaps, and to precise the factors influencing CO_2 patterns and groundwater mineralization in volcanic systems, spatial and temporal evaluation of carbon fates has been carried out in the Argnat basin belonging to the Chaîne des Puys volcanic area (French Massif Central). The interest of this watershed is that the lava flow harbors a high morphological variability, featured by both pahoehoe and a'a lava flows and that these different lava flows are separated. Pahoehoe flows are massive and fissures conducting water are mainly due to thermal effect during lava cooling. In contrast, a'a flows present fissures due to turbulent settlements and injections of porous scoria masses (Self et al. 1998; Kiernan et al. 2003). In addition, this system overlies a fractured substratum potentially degassing mantellic CO_2 (Aubignat 1973; Joux 2002). This could permit to better discriminate the surface influence between these two lava flows. At last, this system allows accessing to the unsaturated zone of the pahoehoe flow, through water catchment galleries.

In this context, a monitoring of carbon-13 of the total dissolved inorganic carbon ($\delta^{13}C_{TDIC}$) and investigations on equilibrating CO_2 pressure (P_{CO_2eq}) which depends on the contribution of the various CO_2 sources, coupled with hydrochemical characterization (major ions), have been carried out during 13 months in 10 outlets (saturated zone; SZ) and one unsaturated zone (UZ). The evaluation of spatial carbon-13 and P_{CO_2eq} patterns was used to identify the potential impact of lava morphologies. The temporal investigation of both UZ and SZ was done to evaluate the hydrometeorological factors influencing the seasonal variability of carbon uptakes by the system.

2 Hydrogeological and Environmental Settings

The Argnat basin is a 26.1 km^2 watershed located in the Chaîne des Puys which is constituted of Upper Pleistocene and Holocene volcanoes that run from north to south over the French Massif Central. The altitude ranges from 380 to 1,159 m with a mean altitude of about 811 m (Fig. 1a).

Five lava flows overly the fractured plutonic basement called "Plateau des Dômes" upstream and "La Limagne" sedimentary downstream (Boivin et al. 2009). These two geological entities are delimited by the Limagne fault. The lava flows originated from different strombolian volcanoes and firstly superimposed in a deep and narrow thalweg cutting the plutonic basement. After the Limagne fault, two lava flows continued but diverged in two different branches: the Grosliers lava flow on south, and the Blanzat flow on north. Further erosion processes led to a relief inversion: Sedimentary terrains overlaid by lava flow have been conserved, whereas surrounding areas have been altered (Fig. 1b). However, a little hill located on northeast of Blanzat has been less affected.

From a chemical point of view, the plutonic substratum mainly consists in granites and syenodiorite (Barbaud 1983). The Limagne basin is composed of marls and calcareous rocks (Boivin et al. 2009). The volcanic rocks are made of alkali basalt and potassic trachybasalt (Boivin et al. 2009) and composed mainly of olivine, K-, and Ca/Na-feldspars (Table 1).

From a morphological point of view, and according to the classification of Macdonald (1953), the Blanzat flow is of an a'a structure, whereas the Grosliers flow presents characteristics that fit with "rubbly pahoehoe" morphology (Fig. 2). A'a lava flows are made of vesicular scoria located at the top and the bottom surrounding a central massive part vertically fissured during the cooling of lava flow (thermal contraction). In contrast, true pahoehoe lava flows are massive and frequently present prisms (Kiernan et al. 2003). Rubbly pahoehoe flows may be considered as a transitional lava type between a'a and pahoehoe. This lava usually presents a smooth and glassy basal zone that often displays joints, a jointed and holocrystalline central zone, and a crustal part. This latter is characterized by a variably preserved and vesicular upper crust associated with a discontinuous layer of flow-top breccias (e.g., Druraiswami et al. 2008).

The surface of strombolian cones and lava flows located up to the Limagne fault are mainly occupied by coniferous and deciduous forest. Near and downward this limit, some villages (Sayat, Malauzat, Blanzat), vineyards (on the Grosliers and the Blanzat lava

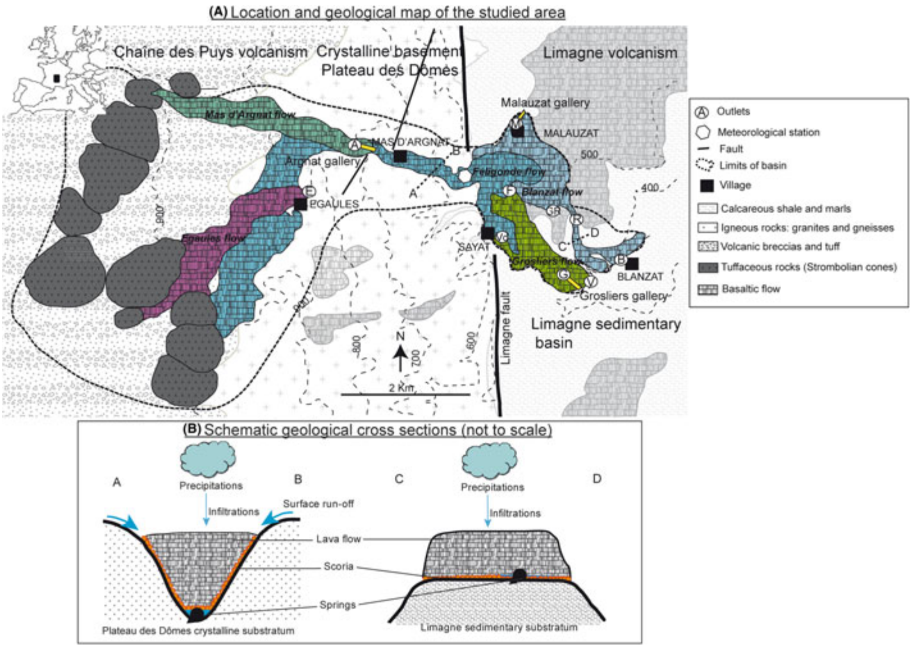

Fig. 1 **a** Location and geological settings of the Argnat basin and localization of the studied outlets, **b** Conceptual scheme of hydrological functioning of lava flows before and after the Limagne fault. *V* Vergnes, *B* Blanzat, *A* Argnat, *E* Egaule, *R* Reilhat catchment, *Vd* Vernède, *F* Féligonde, *M* Malauzat, *GR* Grande source de Reilhat, *G* Grosliers

flows), and crop fields are found. Plutonic terrains are mainly featured by meadows used for livestock rearing.

From a hydrological point of view, Bertrand (2009) estimated the global discharge of the basin being about 300 l/s. Three potential pathways have been described for infiltrated waters (Fig. 1a, b). Precipitation can infiltrate into strombolian cones, composed of clinkers, cinders, and lapilli, that then present at their base a thin (compared with the height of such edifices) saturated zone. This latter recharges the aquifer in the lava flow located downstream, even though such flows are often many kilometers long (Martin-Del Pozzo et al. 2002; Josnin et al. 2007). The recharge may also happen directly on lava flow through scoria, prisms, or inflation fissures (Barbaud 1983; Kiernan et al. 2003). In addition, surface streams circulating over plutonic impermeable substratum may infiltrate into volcanic aquifer at the contact between the basement and the volcanic flows (Hottin et al. 1989). Then, the main groundwater flowpath occurs within the basal scoria zone or in the spoiled zone near the volcanic flow/basement contact (Fig. 1b). Finally, uprising of mineral waters, from fractures affecting the plutonic basement, could partly supply the shallow aquifer (Aubignat 1973; Joux 2002; Livet et al. 2006). Ten springs were sampled for this study (Fig. 1a). Before the Limagne fault, and from upstream to downstream, these outlets are the Egaule catchment and the Argnat gallery which are used as drinking water supply. After the Limagne fault, on the Blanzat flow are located Féligonde and Grande source Reilhat springs, Malauzat gallery, Reilhat borehole, and Blanzat catchment. Les Grosliers gallery (used for industrial water supply), La Vernède, and Les Vergnes springs are associated with the Grosliers flow. Artificial tracer tests done by Belin et al. (1988) or Bertrand (2009) showed that both Blanzat and Grosliers lava flows are hydraulically connected with the Argnat gallery located upstream. In addition, by using oxygen-18 data, Bertrand (2009) estimated that at the annual scale, respectively, for Blanzat and Grosliers system, 50 and 20 % of the discharge come from direct infiltration over the lava flow and partially from runoff over the marly hill located northeast to Blanzat.

Table 1 Chemical compositions of lava flows of the Argnat basin

Lava flow	Blanzat	Grosliers
IUGS Name	Potassic trachybasalt	Subalkali basalt
Orthose	12.41	9.1
Albite	33.85	20.38
Anorthite	22.23	22.7
Nepheline	0	4.41
Di_Wo	0.47	10.15
Di_En	0.27	6.44
Di_Fs	0.19	3.07
En	4	0
Fs	2.79	0
Forsterite	5.49	8.63
Fayalite	4.21	4.54
Mt	4.6	4.58
Ilmenite	4.31	4.39
Apatite	2.11	1.61
Total	96.93	100

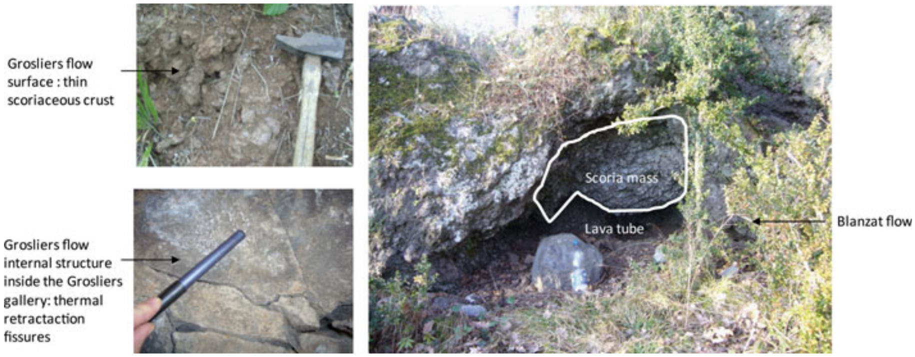

Fig. 2 Field observations of Grosliers and Blanzat flows

3 Methodology

3.1 Sampling

The ten above-mentioned outlets (Fig. 1a) have been sampled at least on a monthly basis between December 2005 and June 2007 for physicochemical measurements and major ions analyses. A monthly sampling for $\delta^{13}C$ measurements was carried out in parallel from April 2006 to April 2007.

Simultaneously, a weekly sampling of both SZ and UZ (infiltrations coming from the little fractures of the gallery roof) of Les Grosliers gallery and the SZ of Argnat gallery has been performed. Precipitation heights and temperature have been measured with a weekly timescale at Sayat meteorological station (Fig. 1a).

Samples were stored at 4 °C in double caps polyethylene bottles for both chemical and isotopic analyses with air-tight seals to prevent atmospheric exchange before isotopic characterization. Taking into account the very low carbon organic contents into Argnat water (determined by previous studies, e.g., Barbaud (1983) and Joux (2002) and confirmed by punctual measurements during the study), samples used for $\delta^{13}C$ analyses were not treated to prevent microbiological and algal bloom.

3.2 Analyses

Electrical conductivity, temperature, and pH measurements as well as concentration in bicarbonates, determined by acidic titration (with a solution of a 0.02 M of H_2SO_4), were performed directly in the field by using a multimeter WTW Multi 340i with a 0.01 pH unity accuracy.

Concentrations of ionic species for the December 2005/June 2007 period were determined by ion chromatography, using a DIONEX DX320 chromatograph with a detection limit (determined by experimentation) of 0.002 mg/l for Cl^- and SO_4^{2-}, 0.007 mg/l for NO_3^-, 0.001 mg/l for Na^+, Mg^{2+}, and Ca^{2+}, and 0.003 mg/l for K^+. The uncertainty of the DX320 chromatograph is 5 %. In order to assess the validity of the sampling device, blanks were tested for the analyzed elements. The highest value was 1.0 µeq/l for sodium and 0.7 µeq/l for calcium; the other elements were not detected. The charge balance (Eq. 1) between anions and cations was assessed, and analyses were considered good for values comprised between -5 and +5 %.

$$\frac{\sum nA^{n-} - \sum nC^{n+}}{\sum nA^{n-} + \sum nC^{n+}} \tag{1}$$

A, C, and n represent, respectively, anions and cations content in mmol l^{-1}, and n is the charge of the ions.

The $\delta^{13}C_{TDIC}$ was measured according to the procedure of Kroopnick et al. (1970). Precipitation of TDIC was obtained by adding NaOH (pH > 12) and $BaCl_2$ in water samples. A precipitate of $BaCO_3$ is obtained and dried. Phosphoric acid is added to the dry $BaCO_3$ sample inside a vacuum line, and the evolved CO_2 is purified and trapped with liquid nitrogen in a glass tube. The isotopic composition of this gaseous CO_2 was then measured with a dual inlet mass spectrometer (Micromass Isoprime). The data are expressed versus the Pee Dee Belemnite (PDB) international standard ($\delta^{13}C = 0$ ‰) as indicated in the Eq. 2. The analytical precision is 0.2 ‰.

$$\begin{aligned} R &= \frac{^{13}\mathrm{C}}{^{12}\mathrm{C}} \\ \delta &= \left[\frac{R_{\mathrm{Sample}}}{R_{\mathrm{standard}}} - 1\right] \times 1000 \end{aligned} \tag{2}$$

3.3 Calculation Approaches

Alteration occurring into crystalline aquifers may be summarized by the equation 3 (Stumm and Morgan 1981; Dessert et al. 2001):

$$\begin{aligned} &\text{Plagioclase} + \text{K-Feldspar} + \text{Olivine} + \text{Pyroxene} + CO_2 + H_2O \rightarrow \\ &[\text{Al} - \text{Si}]\ \text{Minerals} + H_4SiO_4 + HCO_3^- + Ca^{2+}/Mg^{2+}/Na^+/K^+/Sr^{2+} \end{aligned} \tag{3}$$

During this process, cations are released into the water and new aluminosilicates such as kaolinite and smectite may be formed. As shown by Eq. 3, the rock weathering is partly dependant from the CO_2 flux. Its dissolution leads to the formation of TDIC, that is, H_2CO_3, HCO_3^-, CO_3^{2-}, whose proportions are controlled by the temperature and the pH of water (Appelo and Postma 1994).

Knowledge of P_{CO_2eq} has been shown useful to discriminate sources and processes affecting groundwater mineralization in both SZ and UZ (Joux 2002; Emblanch et al. 2003). Calculation of P_{CO_2eq} is possible by applying Eq. 4:

$$P_{CO_2eq} = \frac{\left(HCO_3^-\right) \times (H^+)}{K_{H_2CO_3}(T) \cdot K_{CO_2}(T)} \tag{4}$$

where (HCO_3^-) and (H^+) are ions activities, $K_{H_2CO_3}(T)$ is the dissociation constant of H_2CO_3, and $K_{CO_2}(T)$ is the Henry's constant for dissolution of CO_2. For each sample, calculations were performed by using the Diagramme software (Simler 2003) in which the WATEQ hydrochemical database (Truesdell and Jones 1974) has been implemented. Given that [HCO_3^-] and [H^+] were determined with a pH meter with a 0.01 uncertainty (relative uncertainty: 2.3 %), the propagated uncertainty on the P_{CO_2eq} evaluation is 3.2 % (calculations not shown).

The variability of $\delta^{13}C_{TDIC}$ is due to fractionation factors ε between $\delta^{13}C_{CO_2}$ and $\delta^{13}C_{H_2CO_3}$ or $\delta^{13}C_{HCO_3}$ or $\delta^{13}C_{CO_3}$ (Table 2) and to the signature of the dissolving carbon in waters (Wigley 1975). By taking into account the fractionation factors, it makes it possible to evaluate the initial signature of the CO_2 source which dissolved in water. Inorganic carbon dissolution and speciation may be divided into two steps. At first, water transits from atmosphere to soil and unsaturated zone. In these media, water may be considered as opened to CO_2 since there is not a limited pool of gaseous carbon dioxide. In a system opened to CO_2, the final isotopic signature of the solution is only constrained by gaseous CO_2 phase signature and fractionation factors of speciation as expressed by the Eq. 5 (Wigley 1975; Dever 1985; Rose et al. 1996; Emblanch 1997):

$$\delta^{13}C_{TDIC} = \frac{[H_2CO_3]\left(\delta^{13}C_{CO_2} + \varepsilon_{CO_2-H_2CO_3}\right) + \left[HCO_3^-\right]\left(\delta^{13}C_{CO_2} + \varepsilon_{CO_2-HCO_3^-}\right) + \left[CO_3^{2-}\right]\left(\delta^{13}C_{CO_2} + \varepsilon_{CO_2-CO_3^{2-}}\right)}{[TDIC]} \quad (5)$$

where ε represents the fractionation factor (‰ vs PDB) of the indicated specie with CO_2. $[H_2CO_3]$, $[HCO_3^-]$, and $[CO_3^{2-}]$ are the concentrations of each inorganic carbon species. The values of ε are thermodependant and can be calculated by using the thermodynamic equations reported in Table 2.

Secondly, once the water has reached the saturated zone, then the system may be considered as a closed system regarding CO_2 and hence there is a conservation of the bulk isotopes ratio of TDIC, even if further speciation of the different inorganic species occurs. These processes are also true if water flowing through saturated zone (closed system) temporally meet CO_2 degassing from deep origin (temporally open system).

Consequently, if isotopic signatures acquired in open conditions are then conserved in closed conditions, then it means that by inversing the Eq. 5 and assuming no participation of siliceous rocks in the final signature of $\delta^{13}C_{TDIC}$, the signature of the source of gaseous CO_2 may be evaluated (Eq. 6):

$$\delta^{13}C_{CO_2} = \delta^{13}C_{TDIC} - \frac{\varepsilon_{CO_2-H_2CO_3}[H_2CO_3] + \varepsilon_{CO_2-HCO_3^-}\left[HCO_3^-\right] + \varepsilon_{CO_2-CO_3^{2-}}\left[CO_3^{2-}\right]}{[TDIC]} \quad (6)$$

4 Results and Discussion

4.1 Potential CO_2 Origins in the Hydrogeological System

Statistics of physicochemical and chemical parameters (Dec 05–June 07), $\delta^{13}C_{TDIC}$ (April 06–April 07 period) of the 10 outlets, are presented in Table 3. Raw data are available by consulting Bertrand (2009).

Table 2 Fractionation factors calculation in TDIC

Fractionation factor	Equation	Reference
$\varepsilon^{13}C_{CO_2(aq)-CO_2(g)}$	$10^3 \ln\alpha^{13}C_{CO_2(aq)-CO_2(g)} = -0.373(10^3 \times T^{-1}) + 0.19$	Vogel et al. 1970
$\varepsilon^{13}C_{HCO_3-CO_2(g)}$	$10^3 \ln\alpha^{13}C_{HCO_3-CO_2(g)} = 9.552(10^3 \times T^{-1}) - 24.10$	Mook et al. 1974
$\varepsilon^{13}C_{CO_3-CO_2(g)}$	$10^3 \ln\alpha^{13}C_{CO_3-CO_2(g)} = 0.87(10^6 \times T^{-2}) - 3.4$	Deines et al. 1974
$\varepsilon^{13}C_{CO_2(g)-CaCO_3}$	$10^3 \ln\alpha^{13}C_{CO_2(g)-CaCO_3} = -2.988(10^6 \times T^{-2}) + 7.6663(10^3 \times T^{-1}) - 2.4642$	Bottinga 1968

In order to help the discussion of results, a brief review of the various carbon sources potentially implied in the system and their isotopic characteristics is proposed. Three origins of gaseous CO_2 with different carbon-13 signatures may exist (Alley 1993; Amiotte-Suchet et al. 1999; Gal and Gadalia 2011): (1) incorporation of atmospheric CO_2 before infiltration, (2) soil CO_2 dissolution during surface-underground transfer, and (3) mantellic degassing. Atmospheric $\delta^{13}C_{CO_2}$ was evaluated to be −8 ‰ as an average in the North Hemisphere (Cerling et al. 1991; Levin et al. 1995). This value is slightly different from the value of −7 ‰ of the natural background because of the CO_2 degassing from fossil organic matter combustion. The average of atmospheric P_{CO_2} is known to be around 3.8×10^{-4} atm during the 2000-2010 period (NOAA 2011). Soil $\delta^{13}C_{CO_2}$ is close to the $\delta^{13}C$ characterizing the biologic contributors (Amundson et al. 1998). In temperate climate, mainly featured by plant harboring Calvin C_3 cycle for sugar metabolism (Deines 1980) such as on the Argnat basin, the isotopic signatures of CO_2 into the soil range from −22.5 to −21 ‰ (Rightmire 1978; Batiot 2002; Emblanch 1997; Dever 1985). Soil P_{CO_2} may be very variable, according to climate, depth of soil, and season but usually ranges between 10 and 100 times atmospheric levels (Berthelin 1988). Mantellic gas emissions are a likely source of groundwater DIC in regions of active volcanism (e.g., Federico et al. 2002). The signature of mantellic CO_2 degassed in the Chaîne des Puys was determined to be -6.6 ± 0.8 $\delta^{13}C$ ‰ (Batard et al. 1982). P_{CO_2} is expected to vary with mantellic activity and connection between deep and superficial geological systems. Signatures of the marls and calcareous rocks from La Limagne terrains are close to 0 ‰ because of their marine formation (Bréhérét et al. 2008; Jiráková et al. 2010).

$\delta^{13}C_{TDIC}$ spatially vary and range from -17.5 ± 1.6 ‰ (Egaule) to -9.4 ± 1.1 ‰ (Argnat). The calculation of the mean isotopic signature of dissolving CO_2 (Eq. 6) for each outlet (Table 3) shows that Argnat presents the most enriched value $\left(\delta^{13}C_{CO_2 mean} = -14.2 \pm 1.0\,‰\right)$ in comparison with other catchments. This is consistent with a regional CO_2 degassing mentioned by Camus et al. (1993) and agrees with the proximity of tectonic faults affecting the substratum in the vicinity of Argnat (Boivin et al. 2009; Fig. 1a). It has to be noted that no temperature and EC anomaly was detected during the entire monitoring ($T_{mean} = 8.6 \pm 0.07$ °C et $EC_{mean} = 210 \pm 2$ µS/cm), arguing for the absence of mixing with hydrothermal waters but rather for a diffuse gaseous source. Downstream, two groups of water may be delineated. Firstly, La Vernède (-17.2 ± 1.2 $\delta^{13}C$ ‰), Les Grosliers (-19.4 ± 1.3 $\delta^{13}C$ ‰), and Les Vergnes (-18.6 ± 1.5 $\delta^{13}C$ ‰), which belong to the pahoehoe Grosliers flow. These intermediate values argue for a still significant mantellic CO_2 contribution, or for an atmospheric influence. The second group of waters present contrasting values with Blanzat (-21.4 ± 1.1 ‰), Grande Source Reilhat (-20.7 ± 1.1 ‰), Reilhat borehole (-22.0 ± 1.1 ‰), Malauzat (-22.8 ± 1.7 ‰), and Féligonde (-21.6 ± 1.1 ‰) whose $\delta^{13}C_{CO_2}$ are close to soil signature (e.g., Rightmire 1978). It has also to be noted that Blanzat $\delta^{13}C_{CO_2}$ is not influenced by the probable participation of the marly hill located northeast to the outlet. This is likely due to a circulation occurring in a medium opened to the gaseous CO_2, that is, a superficial circulation. Indeed, in opened conditions, the $\delta^{13}C_{CaCO3}$ of rock materials, close to 0 ‰, is occulted by the gaseous pool (Wigley 1975; Emblanch 1997).

In order to delineate the possible influence of hydrometeorological and geomorphologic parameters on the CO_2 origin in the system, two distinct approaches were carried out and are presented in the following. At first, the hydrometeorological factors will be addressed by combining $\delta^{13}C_{CO_2}$ signatures and $P_{CO_2 eq}$ calculations with a temporal approach in both SZ and UZ of the Grosliers gallery. Secondly, the geomorphologic influence will be

Table 3 Statistics of groundwater chemical (Dec 05–June 07 period) and isotopic (April 06–April 07) data: main variables (pH, temperature, electrical conductivity) major ions, and carbone-13 composition of TDIC

	T °C	E.C. (25 °C) μS cm^{-1}	pH	SiO_2 mg l^{-1}	HCO_3^- mg l^{-1}	Cl^- mg l^{-1}	NO_3^- mg l^{-1}	SO_4^{2-} mg l^{-1}	Na^+ mg l^{-1}	K^+ mg l^{-1}	Mg^{2+} mg l^{-1}	Ca^{2+} mg l^{-1}	$\delta^{13}C_{TDIC}$ (‰ v-PDB)	$\delta^{13}C_{CO_2}$ (‰ v-PDB)	P_{CO_2eq} (atm)
Grosliers U.Z. ($n = 79$)															
Mean	N.d.	205	7.4	46	112.2	4.1	3.7	4.9	15.3	6.8	9.1	13.6	−12.9	−20.6	5.7E−03
SD	N.d.	24	0.2	4	20.8	0.2	0.2	0.2	1.3	0.6	1.8	2.8	1.3	1.1	2.7E−03
Min	N.d.	175	7.1	34	85.4	3.8	3.3	4.4	13.3	5.8	6.8	9.8	−16.7	−23.8	1.2E−03
Median	N.d.	196	7.4	46	102.5	4.1	3.7	4.9	14.9	6.7	8.4	12.9	−13.0	−20.8	5.1E−03
Max	N.d.	256	8.0	57	158.6	4.7	4.2	5.3	18.7	8.1	13.6	20.4	−9.4	−17.3	1.2E−02
Grosliers S.Z. ($n = 79$)															
Mean	10.3	258	7.2	36	83.5	21.5	12.5	12.0	14.6	8.0	11.2	16.3	−12.5	−19.5	8.3E−03
SD	0.0	7	0.4	3	4.2	1.4	0.6	0.5	0.4	0.4	0.6	1.2	1.2	1.3	3.3E−03
Min	10.3	244	6.6	28	75.6	19.0	11.2	11.1	13.7	7.3	9.6	13.3	−17.0	−23.7	1.3E−03
Median	10.3	258	7.0	36	83.0	21.5	12.4	12.0	14.6	7.9	11.1	16.3	−12.3	−19.4	8.9E−03
Max	10.3	273	7.9	45	93.9	25.1	13.9	13.5	15.7	9.4	12.3	18.5	−9.7	−17.4	1.5E−02
Egaule ($n = 19$)															
Mean	8.7	135	6.9	22	50.2	8.5	4.5	8.2	6.0	2.2	4.9	12.9	−17.5	−23.6	6.2E−03
SD	0.3	11	0.3	3	6.8	1.3	1.0	0.9	0.4	0.3	0.6	2.0	1.6	1.9	2.9E−03
Min	7.9	117	6.5	16	41.5	6.3	3.2	6.7	5.3	1.7	4.2	10.3	−20.3	−27.0	9.5E−04
Median	8.8	133	6.9	23	48.8	8.3	4.3	8.4	6.0	2.2	4.8	12.4	−17.4	−23.0	5.8E−03
Max	9.0	159	7.6	29	61.0	11.4	7.1	9.7	7.1	2.7	6.2	16.9	−15.0	−21.0	1.2E−02
Argnat ($n = 19$)															
Mean	8.6	210	6.7	36	80.6	14.1	6.8	8.2	13.0	6.9	9.2	13.2	−9.4	−14.2	1.6E−02
SD	0.1	2	0.2	2	3.7	0.4	0.3	0.4	0.4	0.3	0.4	1.3	1.1	1.0	4.5E−03
Min	8.3	205	6.5	31	73.2	13.4	5.7	7.6	12.5	6.5	8.5	11.4	−11.1	−16.0	8.0E−03
Median	8.6	210	6.7	37	80.5	14.2	6.8	8.2	12.9	7.0	9.2	13.2	−9.3	−13.9	1.4E−02
Max	8.6	213	7.3	39	90.3	14.8	7.2	9.1	14.2	7.5	10.1	16.3	−6.8	−12.2	2.4E−02
Féligonde ($n = 19$)															
Mean	9.9	238	7.3	34	78.6	20.7	11.0	10.0	14.9	7.3	9.8	15.0	−14.5	−21.6	5.0E−03

Table 3 continued

	T °C	E.C. (25 °C) µS cm^{-1}	pH	SiO_2 mg l^{-1}	HCO_3^- mg l^{-1}	Cl^- mg l^{-1}	NO_3^- mg l^{-1}	SO_4^{2-} mg l^{-1}	Na^+ mg l^{-1}	K^+ mg l^{-1}	Mg^{2+} mg l^{-1}	Ca^{2+} mg l^{-1}	$\delta^{13}C_{TDIC}$ (‰ v-PDB)	$\delta^{13}C_{CO_2}$ (‰ v-PDB)	P_{CO_2eq} (atm)
SD	0.5	11	0.3	4	6.7	2.9	1.6	0.3	0.9	0.3	0.8	1.8	1.2	1.1	1.8E−03
Min	8.9	221	6.9	26	68.3	17.2	8.8	9.2	13.7	6.7	8.6	12.5	−16.8	−23.7	9.0E−04
Median	9.9	238	7.2	34	79.3	19.7	10.5	10.1	14.8	7.3	9.8	14.7	−14.4	−21.4	4.8E−03
Max	11.5	263	7.8	41	92.7	28.5	13.6	10.5	16.9	8.0	10.8	17.7	−11.9	−19.9	8.3E−03
Malauzat (n = 19)															
Mean	10.2	421	7.2	45	101.5	49.1	31.7	16.8	22.0	13.0	17.2	29.1	−16.0	−22.8	8.3E−03
SD	0.3	14	0.4	5	9.4	3.9	3.4	0.8	1.7	1.9	1.4	2.9	1.4	1.7	4.3E−03
Min	9.7	401	6.7	35	80.5	42.8	25.7	15.1	20.2	10.7	15.1	25.4	−19.5	−26.5	2.5E−03
Median	10.1	420	7.1	45	102.5	48.9	30.6	16.7	21.6	13.2	16.8	28.7	−15.9	−23.1	7.0E−03
Max	10.8	459	8.0	54	109.8	56.5	39.4	18.1	25.1	17.2	19.4	33.4	−13.4	−19.3	1.6E−02
Reilhat catch. (n = 18)															
Mean	10.7	309	7.3	36	89.8	21.9	31.1	13.3	15.8	8.3	13.7	20.7	−15.1	−22.0	7.1E−03
SD	0.6	18	0.4	2	10.2	1.8	5.7	0.9	0.8	0.4	1.5	3.1	1.0	1.1	2.7E−03
Min	9.3	272	6.9	31	73.2	19.8	19.1	11.6	14.7	7.4	11.4	16.2	−17.3	−24.5	1.7E−03
Median	10.8	314	7.1	36	91.5	21.2	30.5	13.4	15.7	8.3	13.9	21.0	−14.9	−21.8	6.3E−03
Max	11.6	333	8.3	39	108.6	25.9	42.4	15.2	17.2	9.0	16.4	26.6	−13.7	−20.8	1.1E−02
Vernède (n = 19)															
Mean	9.6	232	6.9	36	75.8	20.9	9.5	9.6	15.0	7.1	9.6	14.5	−11.5	−17.2	1.1E−02
SD	0.2	8	0.2	4	4.7	2.7	0.9	0.3	0.7	0.5	0.6	1.5	1.0	1.2	5.8E−03
Min	9.1	221	6.3	30	68.3	17.3	8.3	9.2	13.7	6.4	8.7	12.1	−13.5	−19.1	3.6E−03
Median	9.5	229	6.9	35	73.2	20.3	9.2	9.5	15.0	7.0	9.5	14.5	−11.7	−16.9	9.4E−03
Max	9.9	255	7.3	48	86.6	28.3	11.1	10.3	16.7	8.2	10.9	17.2	−10.2	−15.2	2.9E−02
Vergnes (n = 19)															
Mean	10.0	244	7.3	35	85.5	19.8	10.3	10.3	14.1	7.5	10.8	15.6	−11.4	−18.6	5.6E−03
SD	0.2	5	0.3	3	5.4	1.0	0.4	0.4	0.4	0.4	0.7	1.7	1.1	1.5	2.4E−03
Min	9.6	239	6.8	29	78.1	18.4	9.5	9.3	12.9	7.0	9.7	13.0	−14.2	−22.5	1.9E−03
Median	10.0	244	7.2	35	85.4	19.7	10.3	10.3	14.2	7.4	10.5	15.1	−11.3	−18.1	5.6E−03

Table 3 continued

	T °C	E.C. (25 °C) μS cm^{-1}	pH	SiO_2 mg l^{-1}	HCO_3^- mg l^{-1}	Cl^- mg l^{-1}	NO_3^- mg l^{-1}	SO_4^{2-} mg l^{-1}	Na^+ mg l^{-1}	K^+ mg l^{-1}	Mg^{2+} mg l^{-1}	Ca^{2+} mg l^{-1}	$\delta^{13}C_{TDIC}$ (‰ v-PDB)	$\delta^{13}C_{CO_2}$ (‰ v-PDB)	P_{CO_2eq} (atm)
Max	10.3	253	8.1	42	97.6	21.9	10.9	11.2	14.7	8.2	12.3	18.6	−10.3	−16.6	1.1E−02
Blanzat ($n = 19$)															
Mean	11.7	404	7.1	37	150.8	25.8	28.3	19.7	20.1	8.7	18.5	32.6	−14.7	−21.4	1.3E−02
SD	0.6	20	0.2	3	7.6	1.8	3.1	1.2	1.5	0.5	1.4	2.6	0.6	1.1	5.1E−03
Min	10.0	365	6.7	28	134.2	22.8	23.1	17.7	17.9	8.0	16.0	28.0	−15.6	−22.9	4.0E−03
Median	11.8	410	7.0	36	150.1	26.3	29.1	19.8	20.0	8.6	18.3	32.3	−14.8	−21.5	1.2E−02
Max	12.5	424	7.4	42	165.9	28.6	33.9	21.9	24.0	9.5	20.8	37.1	−13.4	−19.5	2.4E−02
Reilhat G.S. ($n = 15$)															
Mean	10.1	264	6.9	33	82.5	21.7	18.3	11.2	15.0	8.0	11.1	16.9	−14.3	−20.7	8.6E−03
SD	0.0	6	0.2	5	7.7	2.0	1.2	0.5	1.6	1.5	1.1	2.0	0.8	1.1	5.3E−03
Min	10.1	251	6.7	21	70.8	19.3	16.1	10.5	10.0	7.1	7.8	11.2	−15.9	−22.9	1.1E−03
Median	10.1	263	6.9	34	83.0	21.2	18.4	11.0	15.2	7.7	11.2	17.4	−14.4	−20.7	9.0E−03
Max	10.2	276	7.7	40	95.2	25.9	20.4	12.2	16.7	13.2	12.5	19.2	−13.2	−18.8	2.4E−02

investigated through the combination of the same parameters with hydrochemical data throughout the basin.

4.2 Temporal Investigations of Carbon Patterns Throughout the Argnat Basin: Influence of the Hydrometeorological Factors?

The temporal monitorings of Argnat SZ, and Les Grosliers SZ and UZ were carried out to assess which seasonal factors are contributing to the mineralization variability along upstream–downstream (Argnat-Grosliers SZs) and vertical (Grosliers UZ–SZ) water flowpaths in the system. In this purpose, P_{CO_2eq} and $\delta^{13}C_{CO_2}$ were calculated from field data by applying Eqs. 4 and 6 for the period April 06–April 07 (Fig. 3). The hydrometeorological context of measurements is indicated through precipitation heights and temperature compiled on a weekly basis, and the discharge of the Argnat gallery.

Argnat SZ P_{CO_2eq} ranges from 1.0×10^{-2} to 3.5×10^{-2} atm. (Fig. 3b). Except for the 15–21/06/06 week, $\left(\delta^{13}C_{CO_2} = -12.2\delta^{13}C‰\right)$ carbon-13 signatures are rather stable $\left(\delta^{13}C_{CO_2} = -14.2 \pm 1.0\,\delta^{13}C‰\right)$ over the year and range from −16.0 to −13.3 δ^{13}C ‰. High mean P_{CO_2eq} (1.56×10^{-2} atm.) combined with enriched calculated $\delta^{13}C_{CO_2}$ suggest a mixing between deep and biogenic CO_2, as previously mentioned. Between April-06 and October-06, the P_{CO_2eq} has a slight trend to increase. From October-06 (corresponding to the beginning of the weekly monitoring of the gallery), P_{CO_2eq} still increases but presents punctual large variations ($2.2 \times 10^{-2} < P_{CO_2eq} < 3.4 \times 10^{-2}$ atm.).

In the SZ of Les Grosliers (Fig. 3c), P_{CO_2eq} significantly increases from 1.3×10^{-3} to 1.1×10^{-2} atm. between April and October 06. This trend is rather accompanied by a $\delta^{13}C_{CO_2}$ decrease between June and October 06. In contrast, the simultaneous increase of P_{CO_2eq} and $\delta^{13}C_{CO_2}$ from October 06 to April 07 seems to confirm a larger contribution of the mantellic source for this period.

Les Grosliers UZ (Fig. 3d) shows a contrasting behavior with clear seasonal variations of both P_{CO_2eq} and $\delta^{13}C_{CO_2}$. Values of $\delta^{13}C_{CO_2}$ range from −17.3 to −23.8 ‰ and indicate a major biogenic contribution. Between April-06 and October-06, when P_{CO_2eq} increases, $\delta^{13}C_{CO_2}$ decreases, whereas an opposite trend occurs from October-06 to April-07. These seasonal behaviors suggest that temperature controls CO_2 pressure and isotopic signatures in the UZ.

4.2.1 Biogenic Versus Mantellic Contribution in Saturated Zone

These observations imply that CO_2 fluxes and signatures variability in the systems should be altered by time-changing processes. The UZ data showing strong covariations with temperature rather suggest superficial process influences related to weather conditions. These hypothesizes will be discussed in the following.

In contrast, CO_2 fluxes in the Argnat and Grosliers SZ might be modified by changes in mantellic/biogenic proportions depending on fluxes of deep CO_2 or on fluxes of groundwater in equilibrium with biogenic CO_2. In both the SZs, the differences between April and September 06 and from October 06 to April 07 periods could be in agreement with an influence of runoff over hillsides located on each side of lava flows (Fig. 1b). Indeed, the April–September 06 period was more humid than the October 06–April 07 (precipitations heights of 641 and 321 mm, respectively), and the discharge higher (Fig. 3a), consistently with a runoff influence through substratum-lava flow contact. These hillside contributions

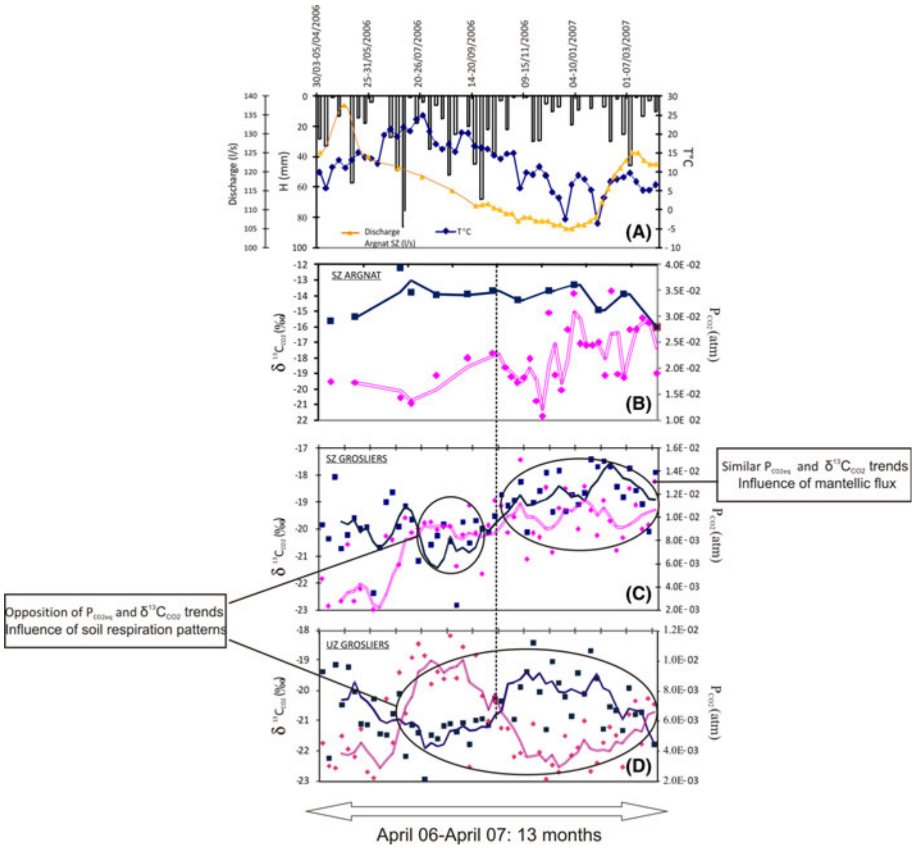

Fig. 3 **a** Temporal evolutions of air temperature and precipitation heights at the meteorological station of Sayat (weekly averaged) and Argnat gallery discharge (after Bertrand 2009). **b–d** $\delta^{13}C_{CO_2}$ and equilibrating CO_2 partial pressure in Argnat SZ, Grosliers SZ, and Grosliers UZ, respectively. *Pink* and *blue lines*, respectively, represent mobile average (2 periods) of P_{CO_2eq} and $\delta^{13}C_{CO_2}$. The *dotted line* crossing **a**, **b**, and **c** represents the limit between the warm (April–September 06) and the cold (October 06–April 07) periods

should be higher during wet periods, providing isotopically depleted DIC (soil signature) and provoking simultaneously lower P_{CO_2eq} in the SZs during winter because of a dilution effect due to low soil respiration (Liu et al. 2007). Conversely, higher P_{CO_2eq} (but only if biogenic P_{CO_2} is higher than mantellic P_{CO_2}) should be more probable in summer (as it will be demonstrated through the UZ data discussion in the following). The increase of P_{CO_2eq} in Argnat SZ and Les Grosliers (coupled with the decrease of $\delta^{13}C_{CO_2}$) from June to October 06 may be consistent with this hillside effect. The punctual P_{CO_2eq} decrease in Argnat SZ during winter after some rain events also argues for this phenomenon.

After October, the general co-increase of P_{CO_2eq} and $\delta^{13}C_{CO_2}$ (more obvious for Les Grosliers which was weekly sampled) could be attributed to successive under saturation and saturation of secondary minerals (calcite $CaCO_3$ or dolomite $CaMg(CO_3)_2$). This process leads to time-limited $\delta^{13}C_{CITD}$ depletion when saturation is reached (Clark and Fritz 1997; Hori et al. 2008). However, this hypothesis may be rejected because saturation has never been reached in SZ throughout the year (annual mean saturation indexes −1.5 for calcite and −4 for dolomite as shown by Bertrand 2009). Another possibility would be the fluid pathway modifications. A less important hillside effect (less fresh water coming from soil) would favor an increase of mantellic proportion (higher P_{CO_2eq} and $\delta^{13}C$). This hypothesis is consistent with the precipitation rate and discharge decreases between spring and winter (Fig. 3a). The co-increase of P_{CO_2eq} and $\delta^{13}C_{CO_2}$ after October could also be explained by a raise of mantellic CO_2 flux in the system. The mantellic CO_2 flux increases observed by Lavina and Del Rosso d'Hers (2008) during the sampling period at the Montchal-Moncynère-Pavin system, located 50 km ago in the southern Chaîne des Puys, may support this hypothesis. In addition, some extensometers set in the vicinity of the study site registered deformation of faults in the substratum. Then, slight reactivations of mantellic activity underlying the Chaîne des Puys or to a better connection (larger faults) between deep and surface systems are possible. This phenomenon may, however, not be considered as the signal of a pending volcanic activity in the area (Boivin et al. 2009; Gal and Gadalia 2011). Further use of complementary approaches would help to precise the influence of hydrological conditions or mantellic CO_2 fluxes variability on gaseous contents of waters, for example, by using $^3He/^4He$ ratio or Radon concentrations (e.g., Federico et al. 2002).

4.2.2 Biogenic Versus Atmospheric Contribution in Unsaturated Zone

The contrasting data between Les Grosliers UZ and SZ (Fig. 3c, Fig. 3d) as well as their dependence to temperature are consistent with an influence of soil organisms' respiration (including roots of trees) (Readon et al. 1979; Stumm and Morgan 1981; Hori et al. 2008). During spring and summer, there is a metabolism and respiration increase within the soil. This results in a seasonal increase of soil P_{CO_2}, favoring carbon dioxide dissolution in soil water (see Eqs. 3 and 4), further reaching the UZ.

The $\delta^{13}C_{CO_2}$ increase in UZ during winter may, however, indicate that an enriched source intervenes slightly and temporarily, especially when soil P_{CO_2} is low. This indicates that UZ carbon patterns are related to processes more complex than dissolution of an unchanged isotopic pool of CO_2. Two hypotheses may be proposed to explain these observations. At first, as for SZ (see above), a temporary precipitation of secondary minerals ($CaCO_3$, $CaMg(CO_3)_2$) could lead to a time-limited (during summer) $\delta^{13}C_{CITD}$ depletion (Clark and Fritz 1997; Hori et al. 2008). This hypothesis may be rejected because as in SZ, secondary mineral saturation has never been reached in UZ throughout the year [saturation indexes were always below −0.48 for calcite and −1.6 for dolomite (Bertrand 2009)]. Secondly, isotopic variations of soil CO_2 could have occurred, caused by air density differences between soil and atmosphere through the "natural ventilation" of soil (Toutain and Baubron 1999; Matsuoka et al. 2001). During winter (reduced soil respiration), soil P_{CO_2} decreases. In addition, atmosphere is usually colder and denser than soil air. The combination of these two phenomena may provoke air diffusion from soil to atmosphere (Quinn 1988; Lohila et al. 2007), what would favor an isotopic enrichment of soil CO_2, carbon-13 being less mobile than carbon-12. The enriched soil CO_2 may dissolve in soil water further reaching the UZ. Moreover, degassing of $^{12}CO_2$ from the UZ water, due to pressure gradient between aqueous CO_2 and gaseous soil CO_2, might be favored. This should cause a supplementary enrichment in $\delta^{13}C_{TDIC}$. In contrast, the summery intense soil respiration favors the increase in soil pressure. In parallel, the air density decreases. This avoids both aerial gases penetration and groundwater degassing and consecutive isotopic modifications (Hori et al. 2008).

Amiotte-Suchet et al. (1999) and Abril et al. (2000) investigated isotopic equilibration between biogenic CO_2 dissolved in rivers and the atmospheric pool of CO_2. They showed that this process only affects the aqueous CO_2 (assumed as H_2CO_3) but not the other carbon species (HCO_3^-, CO_3^{2-}). Hence, in order to assess the influence of atmosphere on the dynamic exchange with soil and unsaturated zone, the so-called "partial isotopic equilibration" was modeled (Eq. 6) and compared with the $\delta^{13}C_{CITD}$ data of Les Grosliers UZ. In this equation, $\delta^{13}C$ is assumed to be −8 ‰ (atmospheric) for the CO_2 leading to the H_2CO_3 signature (equilibration), whereas $\delta^{13}C$ of CO_2 source for bicarbonates and carbonates was assumed to be −21 ‰ (biogenic) The above discussed temperature dependence of soil-atmosphere CO_2 exchanges (Matsuoka et al. 2001) was taken into account: Partial isotopic equilibration with atmospheric CO_2 was presumed only when weekly air temperature was lower than temperature of Les Grosliers gallery ($T = 10.3$ °C over the year) authorizing atmosphere-soil exchanges. When air was warmer, no partial isotopic equilibration was assumed. The results of this simulation (Fig. 4) allow performing the best fittings for the cold periods between 12/10/2006 and 23/11/2006 and between 29/11/2006 and 25/01/2007 (modeled values without equilibration may be found in Bertrand 2009). During this period, the weekly mean air temperature ranged between −2.6 and 9.7 °C, except during the week 23–29/11/2006, (mean $T_{air} = 11.2$ °C); thus, only the soil CO_2 influence was hypothesized for this week. The good fit for cold weeks is consistent with the observations obtained by Karberg et al. (2005), which demonstrated the enrichment of $\delta^{13}C$ of TDIC in natural ecosystems submitted to high atmospheric P_{CO_2}. The simulation is conversely not satisfying for the weeks between 26/01 and 04/04/2007 (−3.8 °C < T_{air} < 9.6 °C) (not shown in the figure). The first week of this period was the coldest week of the campaign (T°_{air} 25 au 31/1/07 = −3.8 °C) and was marked by a remaining of snow cover until mid-February. Dudziak and Halas (1996) indicated that the snow cover and the soil freezing may constitute a thermal barrier between soil and atmosphere as well as a barrier for gas migration. Moreover, snow melt provokes increase in soil P_{CO_2} because new water supplies tend to stimulate soil respiration (Bleak 1970; Coxon and Parkinson 1987). This leads to a typical biogenic signature of $\delta^{13}C_{CO_2}$. Accordingly, a better fit was obtained with a purely biogenic CO_2 source for this cold (frozen) period. Thus, a model of the seasonal CO_2 fates in the UZ of Les Grosliers, which takes into account local weather patterns and soil conditions (snow covered or not), may be proposed (Fig. 5). This provides new insights of the potential seasonal participation of basaltic pahoehoe flows weathering in fixation of atmospheric carbon. The air temperature difference between atmospheric and basaltic compartment should be taken into account to refine C patterns models in such environments.

4.3 Influence of Lavas' Morphological Factor?

Grosliers SZ and UZ harbor contrasting $\delta^{13}C_{CO_2}$ and P_{CO_2eq} temporal evolutions. This suggests a limited influence of the UZ to the SZ of the Grosliers pahoehoe flow. This is in agreement with Bertrand et al. (2010) which compared $\delta^{18}O$ tracers in rain, UZ, and SZ waters. As mentioned previously, the biogenic signatures of Grosliers groundwater thus should be mainly due to hillsides runoff before the Limagne fault (Fig. 1b). This process also affects the Blanzat flow groundwaters (Fig. 6a). However, these latter samples are more influenced by the biogenic CO_2 (see the more depleted $\delta^{13}C_{CO_2}$ Fig. 6a). This highlights the influence of additional processes occurring after the Limagne faults, that is, only in the UZ. Similarly, a bimodal hydrochemical distribution between the a'a Blanzat

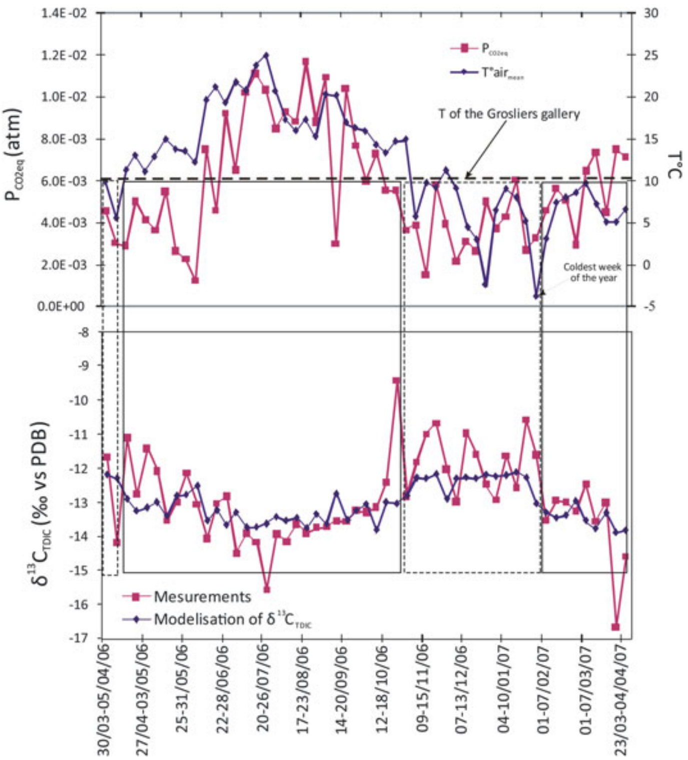

Fig. 4 Evolution of air temperature, P_{CO_2eq}, of measured and calculated $\delta^{13}C_{CITD}$ by considering CO_2 biogenic and atmospheric origin in Grosliers UZ. Calculation with partial equilibration with atmospheric CO_2 is for periods delineated by *dot line squares*. Calculation without partial equilibration is for periods in *full line squares*

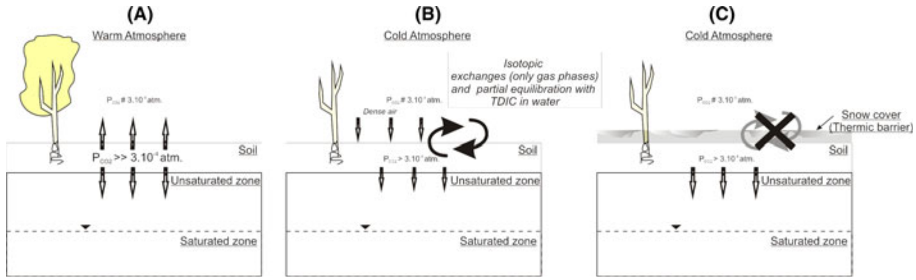

Fig. 5 Conceptual scheme of gaseous CO_2 pattern in atmosphere, soil, and UZ under various meteorological conditions. **a** Warm period: P_{CO_2} is much higher in the soil than in the atmosphere, leading to carbon dioxide diffusion; **b** Cold period: Soil P_{CO_2} decreases. Even if the pressure remains higher than in the atmosphere, the density of cold air allows isotopic exchanges with soil CO_2; **c** Cold period with snow cover: Snow cover and frozen soil limits soil-atmosphere exchanges until snow thawing

flow and the pahoehoe Grosliers flow outlets may be found (Fig. 6b). General increases of alteration (Ca^{2+}, Mg^{2+}, Na^{+}, K^{+}, and HCO_3^{-}) and anthropogenic (Cl^{-}, SO_4^{2-}, and NO_3^{-}) elements concentrations are observed from local rainwater and from upstream to

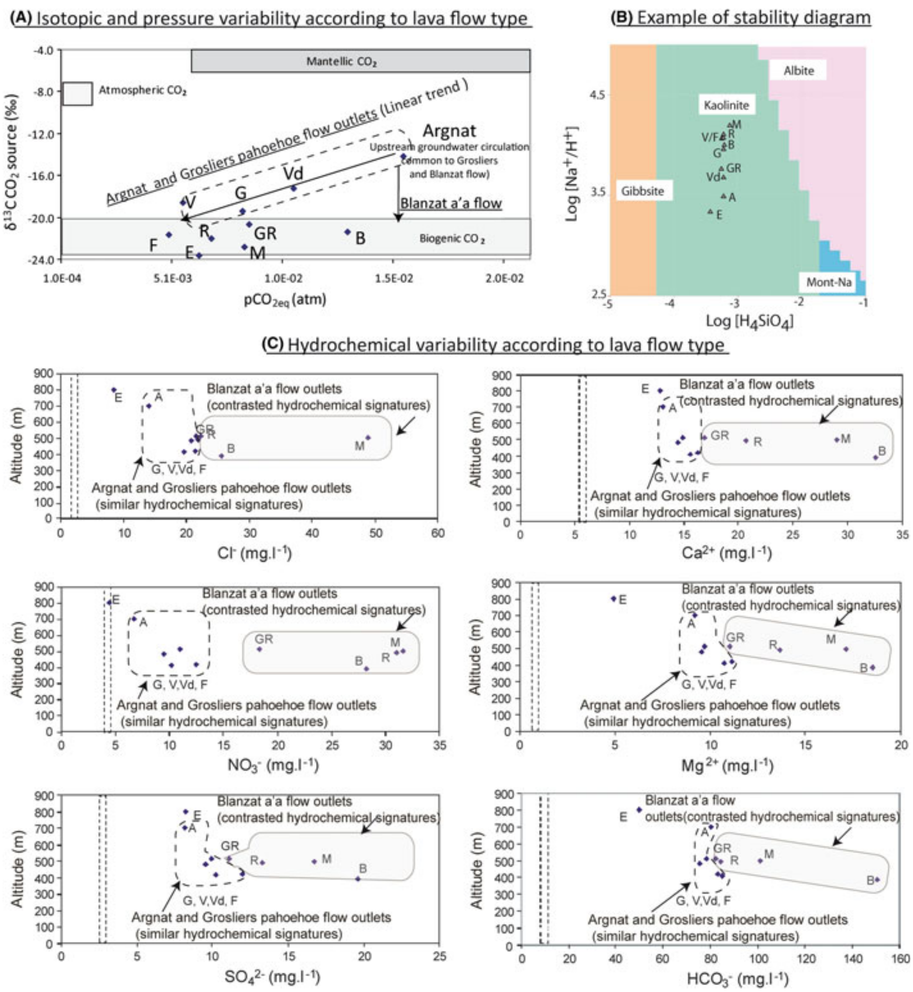

Fig. 6 **a** Spatial evolution of $\delta^{13}C_{CO_2}$ and equilibrating CO_2 partial pressure in the Argnat basin (averaged data for April 2006–April 2007 period). Indicated atmospheric P_{CO_2} is representative of the 2000–2010 period (3.8×10^{-4} atm; NOAA 2011). Biogenic P_{CO_2} range is indicated according to Berthelin (1988). B. Spatial chemical evolution from upstream to downstream. Vertical dashed lines indicate the volume-weighted mean of concentration in efficient precipitations (after Bertrand 2009). C. Example of an obtained stability diagram (using Na^+, H^+, and complexed SiO_2 data. The used thermodynamic data are from the WATEQ database (Truesdell and Jones 1974). *V* Vergnes, *B* Blanzat, *A* Argnat, *E* Egaule, *R* Reilhat catchment, *Vd* Vernède, *F* Féligonde, *M* Malauzat, *GR* Grande source de Reilhat, *G* Grosliers

downstream. The alteration element trends are consistent with the development of weathering processes with increasing residence time (Freeze and Cherry 1979; Dessert et al. 2001, 2003; Cruz and Franca 2006). Progressive enrichment in anthropogenic elements (related to land uses) implies the influence of superficial circulations; as for ^{13}C signatures, they may be partially explained by the runoff from hillsides (Fig. 1b) before the Limagne fault. Beyond these trends, Blanzat outlets generally show higher and more contrasted mineralizations than Grosliers groundwaters, which remain close to the Argnat gallery ones for both alteration and land-use marker elements.

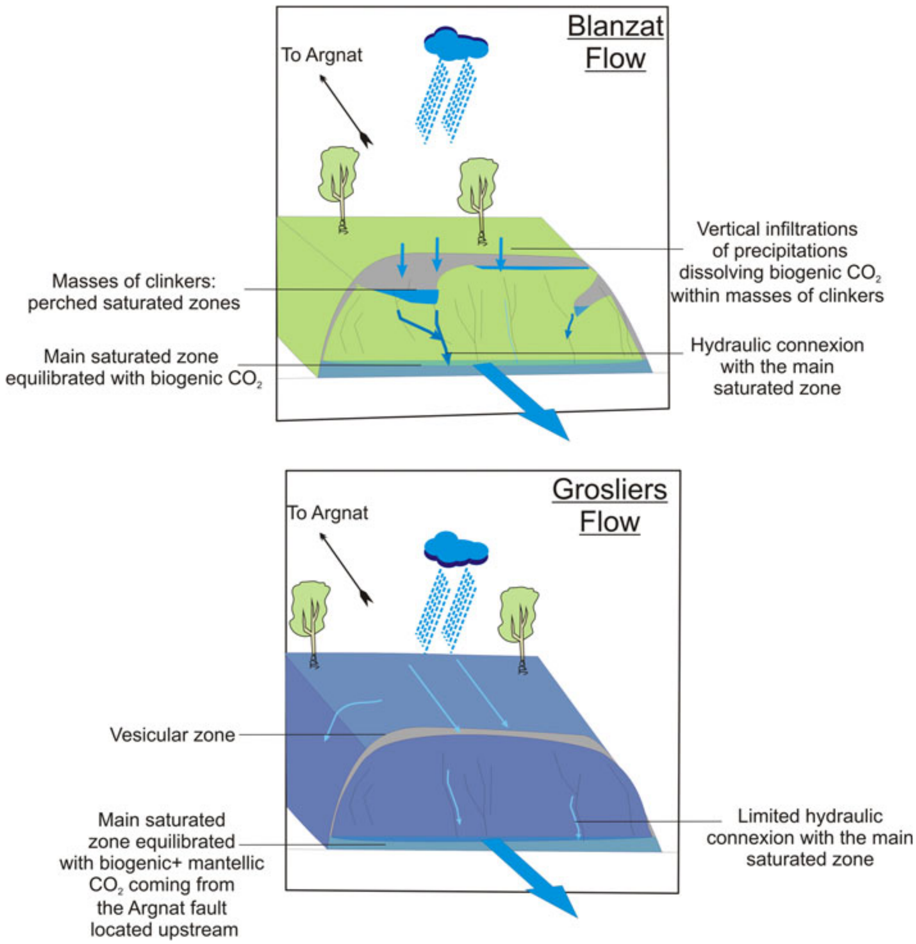

Fig. 7 Conceptual schemes of hydrologic patterns in the a'a Blanzat and pahoehoe Grosliers flows. The fractured and porous structure of a'a flow favors infiltration of water passing through soil. Scoria masses allow storage of water whose TDIC comes from soil respiration. Fractures ensure the hydraulic connection with the main saturated zone located at the contact between lava flow and substratum. In contrast, in rubbly pahoehoe lava flow, the UZ is limited to superficial circulations sparsely connected with the saturated zone

The chemical differences observed between the Grosliers and Blanzat flows are in agreement with the concept of microsystems introduced by Korzhinskii (1959). Microsystems are located at each water–mineral contact and are composed of the primary and secondary minerals and local solutions. Groundwater chemical loadings within a microsystem depend on their category: In so-called open systems (larger fractures), precipitation of gibbsite should be favored, whereas semi-open (in microfractures) and closed systems (primary porosity and microfracture dead ends) are more often related to precipitation of intermediate clay minerals such as kaolinite or smectite and ultimately to equilibrium with primary minerals (e.g., albite, anorthite) (Baynes and Dearman 1978; Sausse et al. 2001; Meunier et al. 2007; Pacheco and Van der Weijden 2012). Stability diagrams (Fig. 6c) show that all the Argnat basin waters are in equilibrium with kaolinite but upstream water (Egaule, Argnat) and pahoehoe Grosliers waters are closer to the gibbsite field in comparison with a'a Blanzat flow waters that tend to be closer to primary minerals. The geometrical heterogeneity of the Blanzat flow is suggested by the fact that some waters emerging from this lava flow (especially at Grande Source Reilhat) are closer to gibbsite stability field. Therefore, the pahoehoe lava flow microsystems in UZ should be rated as an open or semi-open system, whereas the a'a lava flow, featured by numerous microfractures or micro bubbles (Fig. 2), may rather be considered as a patchwork of closed, semi-closed, and open microsystems.

The observed differences in $\delta^{13}C_{CO_2}$ between the Grosliers and the Blanzat flows may also be explained by these geometrical variabilities (Fig. 7). Either UZ water opened to soil CO_2 may reach and significantly participate to the SZ supply or the TDIC already present in water may equilibrate with soil CO_2 (Clark and Fritz 1997) if the system is opened to the gaseous phase (Wigley 1975), that is, in unsaturated conditions. Both the water input and/or gaseous equilibration hypothesizes require that geological structures permit the contact of groundwater systems with a biogenic source of CO_2, that is, that the rocks are sufficiently fractured.

5 Conclusion

This study has demonstrated that $\delta^{13}C$ measurements combined with P_{CO_2eq} calculations, and hydrometeorological and geomorphological evaluations constitute a useful supplement to classical chemical analyses to assess (1) the origins of inorganic carbon in both saturated and unsaturated zones in volcanic systems and (2) the processes of groundwater mineralization.

In the Argnat basin, dissolved carbon may come from biological activities within soil implying respiration, mantellic CO_2 provided through punctual tectonic faults, and temporarily atmospheric CO_2 through UZ during winter, depending on soil activity and micrometeorological conditions of soils.

This work also suggests that water–CO_2–rock interactions strongly depend on the lava flow morphology. Under similar land-use conditions, the geometry of volcanic flows constitutes the major factor influencing groundwater mineralization, because of UZ hydrodynamic variability.

Beyond the Argnat basin case study, these observations argue for the integration of the lava flow morphology in climate, alteration, and global C models involving silicate weatherings as CO_2 sinks (e.g., Amiotte-Suchet and Probst 1995; Amiotte-Suchet et al. 2003). It could also be taken into account for CO_2 sequestration projects in volcanic areas. Indeed, the morphology, by impacting the weathering rate, favors the CO_2 dissolution in carbonates in a'a flows and is less facilitated in pahoehoe flows. When groundwater reaches the surface, the further degassing of CO_2 to atmosphere is more likely for water emerging from pahoehoe systems which should harbor more open microsystems in comparison with a'a lava flows. This information should be useful to evaluate the CO_2 balances between gaseous CO_2 absorption and release by volcanic systems at regional or global scales.

Acknowledgements The authors would like to thank M. Féligonde, the municipalities of Volvic and Blanzat, the Syndicat Basse Limagne, and the ALTEAU Company for their authorizations to access to springs and water supply galleries, and Sébastien Valade and Arnaud Villaros for their help in figure designing. The collaboration with Christophe Rénac for isotopes analyses as well as the comments from Christophe Emblanch on the interpretation of results was much appreciated. They thank Jessica Meeks for her assistance in improving the quality of the text and two anonymous reviewers for their remarks which allowed improvement of this work.

References

Abril G, Etxheber H, Borges AV, Frankignoulle M (2000) Excess atmospheric carbon dioxide transported by rivers into the Scheldt estuary. C R Acad Sci Paris, Sciences de la Terre et des planètes/Earth Planet Sci 330:761–768

Alley WM (1993) Regional ground-water quality. Van Nostrand Reinhold, New York, p 634

Amiotte-Suchet P, Probst JL (1993) Modelling of atmospheric CO_2 consumption by chemical weathering of rocks: application to the Garonne, Congo and Amazon basins. Chem Geol 107:205–210

Amiotte-Suchet P, Probst JL (1995) A global model for present day atmospheric/soil CO_2 consumption by chemical erosion of continental rocks (GEM-CO_2). Tellus 47B:273–280

Amiotte-Suchet P, Aubert D, Probst JL, Gauthier-Lafaye F, Probst A, Andreux F, Viville D (1999) $\delta^{13}C$ pattern of dissolved inorganic carbon in a small granitic catchment : the Strengbach case study Vosges mountains, France. Chem Geol 159:129–145

Amiotte-Suchet P, Probst JL, Ludwig W (2003) Worldwide distribution of continental rock lithology: implications for atmospheric/soil CO_2 uptake by continental weathering and alkalinity river transport to the oceans. Global Biogeochem. Cycles 17 doi:10.1029/2002GB001891 (electronic version)

Amundson R, Stern L, Baisden T, Wang Y (1998) The isotopic composition of soil and soil-respired CO_2. Geoderma 82:83–114

Appelo CAJ, Postma D (1994) Geochemistry, groundwater and pollution. Balkema AA (ed), Rotterdam, p 536

Aubignat A (1973) Le gisement hydrominéral de Volvic en Auvergne [The hydromineral source of Volvic in Auvergne]. Rev Sci Nat Auvergne 39:40–68

Barbaud JY (1983) Etude chimique et isotopique des aquifères du Nord de la Chaîne des Puys. Temps de transit et vulnérabilité des systèmes de Volvic et d'Argnat. PhD thesis, Université d'Avignon, p 209

Batard F, Baudron JC, Bosh B, Marce A, Risler JJ (1982) Isotopic identification of gases of a deep origin in French thermomineral waters. J Hydrol 56:1–21

Batiot C (2002) Etude expérimentale du cycle du carbone en regions karstiques. Apport du carbone organique et du carbone minéral à la connaissance hydrogéologique des systèmes. Site expérimental de Vaucluse, Jura, Larzac, région nord-montpelliéraine, Nerja (Espagne) [Experimental study of the carbon cycle in karstic areas. Contribution of organic and mineral carbons for the hydrogeological understanding of the systems. Experimental sites of Vaucluse, Jura, Larzac, Montpellier's north area, Nerja (Spain)], PhD thesis, Université d'Avignon et des Pays de Vaucluse, p 247

Baynes J, Dearman WR (1978) The microfabric of a chemically weathered granite. Bull Eng Geol Environ 18:91–100. doi:10.1007/BF02635354

Belin JM, Livet M, Heraud H (1988) Autoroute Périgueux Clermont-Ferrand. Dossier d'étude préliminaire de la Chaîne des Puys [Périgueux Clermont-Ferrand Motorway. Preliminary study of the Chaîne des Puys], Ministère de l'équipement et du Logement, CETE Lyon, laboratoire régional de Clermont-Ferrand

Benedetti MF, Menard O, Noack Y, Carvalho A, Nahon D (1994) Water-rock interactions in tropical catchments: field rates of weathering and biomass impact. Chem Geol 118:203–220

Berthelin J (1988) Microbial weathering processes in natural environments. In: Lerman A, Meybeck M (eds) Physical and chemical weathering in geochemical cycles. Kluwer, Dordrecht

Bertrand G (2009) De la pluie à l'eau souterraine. Apport du traçage naturel (ions majeurs, isotopes) à l'étude du fonctionnement des aquifères volcaniques. (Bassin d'Argnat, Auvergne, France) [From rain to groundwater. Contribution of natural tracers (major ions, isotopes) for the study of volcanic aquifer functiuning (Argnat basin, Auvergne, France)]. PhD thesis, University Blaise Pascal Clermont-Ferrand 2, 294 p. Available on: http://tel.archives-ouvertes.fr/docs/00/55/69/10/PDF/25042009_these_GBERTRAND.pdf. Accessed the 05-02-2012

Bertrand G, Celle-Jeanton H, Huneau F, Loock S, Rénac C (2010) Identification of different groundwater flowpaths within volcanic aquifers using natural tracers: influence of lava flows morphology. (Argnat basin, Chaîne des Puys, France). J Hydrol 391:223–234

Bertrand G, Goldscheider N, Gobat JM, Hunkeler D (2012a) Review: from multi-scale conceptualization of groundwater-dependent ecosystems to a classification system for management purposes. Hydrogeol J 20:5–25

Bertrand G, Masini J, Goldscheider N, Meeks J, Lavastre V, Celle-Jeanton H, Gobat JM, Hunkeler D (2012b) Determination of spatio-temporal variability of tree water uptake using stable isotopes ($\delta^{18}O$; $\delta^{2}H$) in an alluvial system supplied by a high-altitude watershed, Pfyn Forest, Switzerland. Ecohydrology, online. doi:10.1002/eco.1347

Bleak AT (1970) Disappearance of plant material under a winter snow cover. Ecology 51:915–917

Bluth GJS, Kump LR (1994) Lithologic and climatic control of river chemistry. Geochim Cosmochim Acta 58:2341–2359
Boivin P, Besson JC, Briot D, Camus G, De Goër De Herve A, Gourgaud A, Labazuy P, De Larouzière FD, Livet M, Mergoil J, Miallier D, Morel JM, Vernet G, Vincent PM (2009) Volcanologie de la Chaîne des Puys, Massif Central Français [Volcanology of the Chaîne des Puys], 5th édn, Editions du parc naturel régional des volcans d'Auvergne
Bottinga Y (1968) Calculation of fractionation factors for carbon and oxygen isotopic exchange in the system calcite-carbon dioxide-water. J Phys Chem 72:800–818
Brady PV, Dorn RI, Brazel AJ, Clark J, Moore RB, Glidewell T (1999) Direct measurement of the combined effects of lichen, rainfall and temperature on silicate weathering. Geochim Cosmochim Acta 63:3293–3300
Bréhérét JG, Fourmont A, Macaire JJ, Negrel P (2008) Microbially mediated carbonates in the Holocene deposits from Sarliève, a small ancient lake of the French Massif Central, testify to the evolution of a restricted environment. Sedimentology 55:557–578
Camus G, Michard GPO, Boivin P (1993) Risque d'éruption gazeuse carbonique en Auvergne [Gaseous carbon eruption risk in Auvergne]. Bull Soc Géol France 164(6):767–781
Carrillo-Rivera JJ, Varsányi I, Kovács L, Cardona A (2007) Tracing groundwater flow systems with hydrogeochemistry in contrasting geological environments. Water Air Soil Pollut 184:77–103
Cerling TE, Solomon DK, Quade J, Borman JR (1991) On the isotopic composition of carbon in soil carbon dioxide. Geochim Cosmochim Acta 55:3403–3405
Charlier JB, Lachassagne P, Ladouche B, Cattan P, Moussa R, Voltz M (2011) Structure and hydrogeological functioning of an insular tropical humid andesitic volcanic watershed: a multi-disciplinary experimental approach. J Hydrol 398:155–170
Chiodini G, Frondini F, Kerrick DM, Rogie J, Parello F, Peruzzi L, Zanzari AR (1999) Quantification of deep CO fluxes from Central Italy. Examples of carbon balance for regional aquifers and of soil diffuse degassing. Chem Geol 159:205–222
Clark ID, Fritz P (1997) Environmental isotopes in hydrogeology. Lewis, New York, p 328
Coxon DS, Parkinson D (1987) Winter respiratory activity in aspen woodland forest floor litter and soils. Soil Biol Biochem 19:49–59
Cruz JV, Amaral CS (2004) Major ion chemistry of groundwater from perched-water bodies of the Azores (Portugal) volcanic archipelago. Appl Geochem 19:445–459
Cruz JV, Franca Z (2006) Hydrogeochemistry of thermal and mineral water springs of the Azores archipelago (Portugal). J Volcanol Geoth Res 151:382–398
Dafny E, Burg A, Gvirtzman H (2006) Deduction of groundwater flow regime in a basaltic aquifer using geochemical and isotopic data: the Golan Heights, Israel case study. J Hydrol 330:506–524
Deines P (1980) The isotopic composition of reduced organic carbon. In: Fritz P, Fontes JC (eds) Handbook of environmental isotope geochemistry, vol 1. Elsevier, New York, pp 329–406
Deines P, Langmuir D, Harmon RS (1974) Stable isotope ratios and the existence of a gas phase in the evolution of carbonate groundwaters. Geochim Cosmochim Acta 38:1147–1154
Demlie M, Wohnlich S, Ayenew T (2008) Major ion hydrochemistry and environmental isotope signatures as a tool in assessing groundwater occurrence and its dynamics in a fractured volcanic aquifer system located within a heavily urbanized catchment, central Ethiopia. J Hydrol 353:175–188
Dessert C, Dupré B, Francois LM, Schott J, Gaillardet J, Chakrapani GJ, Bajpai S (2001) Erosion of Deccan Traps determined by river geochemistry: impact on the global climate and the $^{87}Sr/^{86}Sr$ ratio of seawater. Earth Planet Sci Lett 188:459–474
Dessert C, Dupré B, Gaillardet J, Francois LM, Allegre CJ (2003) Basalt weathering laws and impact of basalt weathering on the global carbon cycle. Chem Geol 202:257–273
Dever ML(1985) Approaches chimiques et isotopiques des interactions fluide-matrice en zone non saturée carbonatée [Chemical and isotopic approaches of fluid-matrix interaction in carbonate saturated zone]. PhD thesis, Université Paris XI, p 196
D'Ozouville N, Auken E, Sorensen K, Violette S, De Marsily G, Deffontaines B, Merlen G (2008) Extensive perched aquifer and structural implications revealed by 3D resistivity mapping in a Galapagos volcano. Earth Planet Sci Lett 269:518–522
Drever JI (1994) The effect of land plants on weathering rates of silicate minerals. Geochim Cosmochim Acta 58:2325–2332
Druraiswami RA, Bondre NR, Managrave S (2008) Morphology of rubbly pahoehoe (simple) flows from the Deccan Volcanic Province: implications for style of emplacement. J Volcanol Geoth Res 177:822–836
Dudziak A, Halas S (1996) Influence of freezing and thawing on the carbon isotope composition in soil CO_2. Geoderma 69:209–216

Edmond JM, Palmer MR, Measures CI, Grant B, Stallard RF (1995) The fluvial geochemistry and denudation rate of the Guyana Shield in Venezuela, Colombia, and Brazil. Geochim Cosmochim Acta 59:3301–3325

Emblanch C (1997) Les équilibres chimiques et isotopiques du carbone dans les aquifères karstiques: étude en région méditerranéenne de montagne [Chemical and isotopic equilibria of carbon in karstic aquifer: study in mountainous Mediterranean area] PhD thesis, Université d'Avignon et des Pays du Vaucluse, p 184

Emblanch C, Zuppi GM, Mudry J, Blavoux B, Batiot C (2003) Carbon 13 of TDIC to quantify the role of the unsaturated zone: the example of the Vaucluse karst systems (Southeastern France). J Hydrol 279(1–4):262–274

European Union Groundwater Directive (2006/118/EC), 2006 Available on: http://ec.europa.eu/environment/water/water-framework/groundwater/policy/current_framework/new_directive_en.htm. Accessed the 05-02-2012

Federico C, Aiuppa A, Allard P, Bellomo S, Jean-Baptiste P, Parello F, Valenza M (2002) Magma-derived gas influx and water-rock interactions in the volcanic aquifer of Mt Vesuvius, Italy. Geochim Cosmochim Acta 66:963–981

Freeze AR, Cherry JA (1979) Groundwater. Prentice-Hall, Englewood Cliffs, NJ, USA, p 604

Gaillardet J, Dupré B, Louvat P, Allègre CJ (1999) Global silicate weathering and CO_2 consumption rates deduced from the chemistry of the large rivers. Chem Geol 159:3–30

Gal F, Gadalia A (2011) Soil gas measurements around the most recent volcanic system of metropolitan France (Lake Pavin, Massif Central). C R Geosci 343:43–54

Garrels RM, Mackenzie F (1971) Evolution of Sedimentary Rocks. Norton, New York

Gislason SR, Arnorsson S, Armannsson H (1996) Chemical weathering of basalt as deduced from the composition of precipitation, rivers and rocks in SW Iceland: effect of runoff, age of rocks and vegetative/glacial cover. Am J Sci 296:837–907

Hinsinger P, Barros ON, Benedetti MF, Noack Y, Callot G (2001) Plant-induced weathering of a basaltic rocks: experimental evidence. Geochim Cosmochim Acta 65:137–152

Hori M, Hoshino K, Okumura K, Kano A (2008) Seasonal patterns of carbon chemistry and isotopes in tufa depositing groundwaters of southwestern Japan. Geochim Cosmochim Acta 72:480–492

Hottin AM, Camus G, Michaeli B, Marchand J, Perichaud J, D'Arcy D (1989) Notice explicative, carte geol. France (1/50000), feuille Pontgibaud (692) [Explicative notice, geological map France (1/50000), sheet of Pontgibaud (692)] Orléans, BRGM, p 103

Jiráková H, Huneau F, Hrkal Z, Celle-Jeanton H, Le Coustumer P (2010) Carbone isotopes to constrain the origin and circulation pattern of groundwater in the north-western part of the Bohemian Cretaceous Basin (Czech Republic). Appl Geochem 25:1265–1279

Josnin JY, Livet M, Besson JC (2007) Characterizing unsaturated flow from packed scoriated lapilli: application to Strombolian cone hydrodynamic behaviour. J Hydrol 335:225–239

Joux M (2002) Structure et fonctionnement hydrogéologique du système aquifère volcanique des eaux minérales de Volvic (Chaîne des Puys, Massif Central Français) [Structure and hydrogeological functiuning of mineral waters of Volvic (Chaîne des Puys, French Massif Central)] PhD thesis, Université d'Avignon et des Pays du Vaucluse, p 227

Karakaya N, Karakaya MC, Nalbantçılar MT, Yavuz F (2007) Relation between spring-water chemistry and hydrothermal alteration in the Şaplıca volcanic rocks, Şebinkarahisar (Giresun, Turkey). J Geochem Explor 93:35–46

Karberg NJ, Pregitzer ÆKS, King ÆJS, Friend AL, Wood ÆJR (2005) Soil carbon dioxide partial pressure and dissolved inorganic carbonate chemistry under elevated carbon dioxide and ozone. Oecologia 142:296–306

Kiernan K, Wood C, Middleton G (2003) Aquifer structure and contamination risk in lava flows: insights from Iceland and Australia. Environ Geol 43:852–865

Kløve B, Ala-aho P, Allan A, Bertrand G, Druzynska E, Ertürk A, Goldscheider N, Henry S, Karakaya N, Karjalainen TP, Koundouri P, Kværner J, Lundberg A, Muotka T, Preda E, Pulido Velázquez M, Schipper P (2011) Groundwater Dependent Ecosystems: part II—ecosystem services and management under risk of climate Change and Land-Use Management. Environ Sci Policy 14:782–793

Korzhinskii DS (1959) Physicochemical basis of the analysis of the paragenesis of minerals (translation). Consultant Bureau, New York, p 143

Kroopnick PM, Deuser WG, Graig H (1970) Carbon-13 measurements on dissolved inorganic carbon in the North Pacific _1969. GEOSECS station. J Geophys Res 75:7668–7671

Kulkarni H, Deolankar SB, Lalwani A (2000) Hydrogeological framework of the Deccan basalt groundwater systems, west-central India. Hydrogeol J 8:368–378

Lavina P, Del Rosso d'Hers T (2008) Le complexe volcanique Montchal-Pavin-Montcynère: nouvelles stratigraphie, tephrochronologie et datations, vers une nouvelle réévaluation de l'aléa volcano-tectonique en Auvergne [The volcanic complex of montchal-Pacin-Montcynère: new stratigraphy, tephrochronology and datations, toward a new evaluation of the volcano-tectonic alea in Auvergne]. XXII^{ème} Réunion des Sciences de la Terre, Nancy, April 2008
Levin I, Graul R, Trivett NBA (1995) Long-term observations of atmospheric CO_2 and carbon isotopes at continental sites in Germany. Tellus 47B:23–34
Liu Z, Li Q, Sun H, Wang J (2007) Seasonal, diurnal and storm-scale hydrochemical variations of typical epikarst springs in subtropical karst areas of SW China:soil CO_2 and dilution effects. J Hydrol 337:207–223
Livet M, D'Arcy A, Dupuy C (2006) Synthèse hydrogéologique de l'Auvergne [Hydrogeological synthesis of Auvergne]. In ''Aquifères et eaux souterraines en France''[Aquifers and groundwaters in France], Ed. BRGM, p 956
Lloret E, Dessert C, Gaillardet J, Albéric P, Crispi O, Chaduteau C, Benedetti MF (2011) Comparison of dissolved inorganic and organic carbon yields and fluxes in the watersheds of tropical volcanic islands, examples from Guadeloupe (French West Indies). Chem Geol 280:65–78
Lohila A, Aurela M, Regina K, Tuovinen JP, Laurila T (2007) Wintertime CO_2 exchange in a boreal agricultural peat soil. Tellus 59B:860–873
Louvat P, Allègre CJ (1997) Present denudation rates at Réunion island determined by river geochemistry: basalt weathering and mass budget between chemical and mechanical erosions. Geochim Cosmochim Acta 61:3645–3669
MacDonald GA (1953) Pahoehoe, a'a and block lava. Am J Sci 251:169–191
Martin-Del Pozzo A, Aceves F, Espinasa R, Aguayo A, Inguaggiato S, Morales P, Cienfuegos E (2002) Influence of volcanic activity on spring water chemistry at Popocatepetl volcano, Mexico. Chem Geol 190:207–229
Matsuoka J, Kano A, Oba T, Watanabe T, Sakai S, Seto K (2001) Seasonal variation of stable isotopic compositions recorded in a laminated tufa, SW Japan. Earth Planet Sci Lett 192:31–44
Matter JM, Takahashi T, Goldberg D (2007) Experimental evaluation of in situ CO_2-water-rock reactions during CO_2 injection in basaltic rocks: implications for geological CO_2 sequestration. Geochem Geophys Geosyst 8:Q02001. doi:10.1029/2006GC001427
Meunier A, Sardini P, Robinet JC, Prêt D (2007) The petrography of weathering processes: facts and outlooks. Clay Miner 42:415–435
Meybeck M (1987) Global chemical weathering of surficial rocks estimated from river dissolved loads. Am J Sci 287:401–428
Millot R, Gaillardet J, Dupré B, Allègre CJ (2002) The global control of silicate weathering rates and the coupling with physical erosion: new insights from rivers of the Canadian Shield. Earth Planet Sci Lett 196:83–98
Mook WG, Groenweld DJ, Brouwn AE, van Ganwijk AJ (1974) Analysis of a run-off hydrograph by means of natural ^{18}O. Conference Proceedings Isotope Techniques in Ground-Water Hydrology, IAEA, Vienna, pp 145–155
Moulton KL, West J, Berner RA (2000) Solute flux and mineral mass balance approaches to the quantification of plant effects on silicate weathering. Am J Sci 300:539–570
National Oceanic and Atmospheric Administration (NOAA) (2011): Mauna Loa Annual Mean CO_2. Available on ftp://ftp.cmdl.noaa.gov/ccg/co2/trends/co2_annmean_mlo.txt. Accessed the 05-02-2012
Négrel P, Allègre CJ, Dupré B, Lewin E (1993) Erosion sources determined by inversion of major and trace element ratios and strontium isotopic ratios in river water: the Congo Basin case. Earth Planet Sci Lett 120:59–76
Nesbitt HW, Wilson RE (1992) Recent chemical weathering of basalts. Am J Sci 292:740–777
Pacheco FAL, Van der Weijden CH (2012) Weathering of plagioclase across variable flow and solute transport regimes. J Hydrol 420–421:46–58
Pokrovsky OS, Schott J, Kudryavtzev DI, Dupré B (2005) Basalt weathering in Central Siberia under permafrost conditions. Geochim Cosmochim Acta 69(24):5659–5680
Quinn JA (1988) Relationship between temperature and radon levels in Lehma Caves, Nevada. US Natl Speleol Soc Bull 50:9–63
Readon EJ, Allison GB, Fritz P (1979) Seasonal chemical and isotopic variations of soil CO2 at Trout Creeg, Ontario. J Hydrol 43:355–371
Rightmire CT (1978) Seasonal variation in pCO_2 and ^{13}C content of soil atmosphere. Water Res 14:691–692
Rose TP, Davisson ML, Criss RE (1996) Isotope hydrology of voluminous cold springs in fractured rock from an active volcanic region, northeastern California. J Hydrol 179:207–236

Sausse J, Jacquot E, Leroy J, Lespinasse M (2001) Evolution of crack permeability during fluid–rock interaction. Example of the Brézouard granite (Vosges, France). Tectonophysics 336:199–214
Self S, Keszthelyi L, Thordarson T (1998) The importance of pāhoehoe. Annu Rev Planet Sci 26:81–110
Simler R (2003) Diagramme software. Available on: http://www.lha.univ-avignon.fr/LHA-Logiciels.htm. Accessed the 05-02-2012
Stallard RF, Edmond JM (1983) Geochemistry of the Amazon: 2. The influence of geology and weathering environment on the dissolved load. J Geophys Res 88(C14):9671–9688
Stefansson A, Gislason SR (2001) Chemical weathering of basalts, Southwest Iceland: effect of rock crystallinity and secondary minerals on chemical fluxes to the oceans. Amer J Sci 301:513–556
Stewart BW, Capo RC, Chadwick OA (2001) Effects of rainfall on weathering rate, base cation provenance, and Sr isotope composition of Hawaiian soils. Geochim Cosmochim Acta 65:1087–1099
Stieljes L (1988) Hydrogéologie de l'île volcanique océanique de Mayotte (archipel des Comores, océan indien occidental) [Hydrogeology of the oceanic volcanic island of Mayotte (Comores archipelgo, occidental Indian ocean)]. Hydrogeol J 2:135–152
Stumm W, Morgan JJ (1981) Aquatic chemistry. Wiley, New York, p 780
Toutain JP, Baubron JC (1999) Gas geochemistry and seismotectonics: a review. Tectonophysics 304:1–27
Truesdell AH, Jones RF (1974) WATEQ, a computer program for calculating chemical equilibria of natural waters. US Geol Survey J Res 2(2):233–274
Violette S, Ledoux E, Goblet P, Carbonnel JP (1997) Hydrologic and thermal modelling of an active volcano: the Piton de la Fournaise, La Réunion Island. J Hydrol 191:37–63
Vogel JC, Grootes PM, Mook WG (1970) Isotope fractionation between gaseous and dissolved carbon dioxide. J Phys 230:255–258
White AF, Blum AE (1995) Effects of climate on chemical weathering in watersheds. Geochim Cosmochim Acta 59:1729–1747
Wigley TML (1975) Carbon 14 dating of groundwater from closed and open systems. Wat Res Res 11(2):324–328